PNAS RESEARCH ARTICLE | NEUROSCIENCE OPEN ACCESS

The acquisition of cold sensitivity during TRPM8 ion channel evolution

Xiancui Lu[a,1], Zhihao Yao[a,1], Yunfei Wang[a,1], Chuanlin Yin[a], Jiameng Li[a], Longhui Chai[a], Wenqi Dong[a], Licheng Yuan[a], Ren Lai[b,c,2], and Shilong Yang[a,2]

Edited by Yifan Cheng, University of California, San Francisco, CA; received January 24, 2022; accepted April 22, 2022

To cope with temperature fluctuations, molecular thermosensors in animals play a pivotal role in accurately sensing ambient temperature. Transient receptor potential melastatin 8 (TRPM8) is the most established cold sensor. In order to understand how the evolutionary forces bestowed TRPM8 with cold sensitivity, insights into both emergence of cold sensing during evolution and the thermodynamic basis of cold activation are needed. Here, we show that the *trpm8* gene evolved by forming and regulating two domains (MHR1-3 and pore domains), thus determining distinct cold-sensitive properties among vertebrate TRPM8 orthologs. The young *trpm8* gene without function can be observed in the closest living relatives of tetrapods (lobe-finned fishes), while the mature MHR1-3 domain with independent cold sensitivity has formed in TRPM8s of amphibians and reptiles to enable channel activation by cold. Furthermore, positive selection in the TRPM8 pore domain that tuned the efficacy of cold activation appeared late among more advanced terrestrial tetrapods. Interestingly, the mature MHR1-3 domain is necessary for the regulatory mechanism of the pore domain in TRPM8 cold activation. Our results reveal the domain-based evolution for TRPM8 functions and suggest that the acquisition of cold sensitivity in TRPM8 facilitated terrestrial adaptation during the water-to-land transition.

TRPM8 | MHR1-3 domain | cold sensitivity | water-to-land transition

Given that temperature influences all biological operations, the evolution of thermosensory adaptation is crucial in shaping the specialized temperature-dependent inhabitation of an organism. At the cellular level, thermosensory neurons in the dorsal root ganglia or trigeminal ganglia innervate the skin and transmit temperature information to the spinal cord and the brain. To bestow such neurons with thermal sensitivity, animals have a toolkit of temperature-sensitive ion channels located on the cell membrane at the molecular level. Accordingly, several members of the transient receptor potential (TRP) superfamily with steep thermosensitivity (referred to as thermoTRP) have attracted the general interest in the field of thermal biology, as they sufficiently cause steep changes in depolarizing currents upon either heating or cooling and thus are considered as the primary molecular sensors of temperature (1–4). Therefore, the evolutionary strategy for directly tuning the thermal activation in thermoTRPs can be employed by animals for their specialized thermosensory adaptation, as seen in vampire bats, pit-bearing snakes, platypus, penguins, squirrels, and camels (5–9).

As heat sensation (warmth and extreme heat) provides the precondition of a fundamental and conserved biological survival process, the genes that encode heat sensors are considered ancient in many metazoan organisms. The annotation of *trpv1* is consistently available in the genomes of fishes, insects, amphibians, reptiles, birds, and mammals. Despite the species-specific temperature-sensitive ranges, a growing number of studies have reported the functional convergence of these heat-sensitive thermoTRP orthologs at the protein level (10), suggesting the essential role of these channels in heat perception across species. Compared to heat sensors, the cold-sensitive thermoTRP likely evolved late. As the most established cold sensor responsive to low temperatures and cooling compounds, transient receptor potential melastatin 8 (TRPM8) was found in somatosensory neurons, and genetic ablation of *trpm8* either in the neurons or mice led to a largely decreased cold sensitivity (4, 11–13). Interestingly, cold activation of amphibian TRPM8 has been tested (14), while sequencing efforts indicated the absence of the *trpm8* gene in 12 fish species from 10 different orders (15). Several specific domains that may alter TRPM8 cold activation have been reported, including the pore domain, voltage sensing apparatus, and C terminus (8, 16–19). Notably, although the efficacy of cold activation is largely altered by residue substitutions in the pore domain, the channel mutants are still cold sensitive (8). Therefore, these findings based on domain/residue swapping among cold-sensitive TRPM8 orthologs may not draw an overall picture in functionally important domains

Significance

Adaptation to more severe ambient temperature fluctuations can be considered one of the key innovations of terrestrial tetrapods. Our study shows the formation of the functional MHR1-3 domain in transient receptor potential melastatin 8 (TRPM8) bestowed the channel with cold sensitivity during the water-to-land transition. The evolved MHR1-3 domain found in terrestrial tetrapods serves as an independent apparatus with cold sensitivity. Furthermore, this domain with independent cold sensitivity is necessary for the regulatory mechanism of the pore domain, where the efficacy of cold activation is largely altered by evolutionary tuning of the hydrophobicity of several residues during the diversification of terrestrial tetrapods. Our findings advance the understanding of cold-sensing emergence during evolution and the thermodynamic basis of TRPM8 cold activation.

Author contributions: R.L. and S.Y. designed research; X.L., Z.Y., Y.W., C.Y., J.L., L.C., W.D., and L.Y. performed research; X.L., Z.Y., and S.Y. contributed new reagents/analytic tools; X.L., Z.Y., Y.W., C.Y., J.L., L.C., W.D., L.Y., and S.Y. analyzed data; and X.L., R.L., and S.Y. wrote the paper.

The authors declare no competing interest.

This article is a PNAS Direct Submission.

[1]X.L., Z.Y., and Y.W. contributed equally to this work.

[2]To whom correspondence may be addressed. Email: rlai@mail.kiz.ac.cn or syang2020@nefu.edu.cn.

This article contains supporting information online at http://www.pnas.org/lookup/suppl/doi:10.1073/pnas.2201349119/-/DCSupplemental.

Published May 20, 2022.

responsible for cold sensitivity. How did the *trpm8* gene originate? How did TRPM8 integrate and modulate cold sensitivity throughout evolution? The answers to such questions probably lead us to understand the evolution of temperature perception and identify the essential structural elements that shape TRPM8 cold activation.

In this study, we show the presence of the young *trpm8* gene in lobe-finned fishes, believed to be the ancestors that gave rise to all land vertebrates (20). Such a young type of *trpm8* derived from the *trpm2* exon shuffling was originated and formed during the expansion of lobe-finned fish genomes. By detecting the positive selection-rich domains, we described the formation of the thermosensitive MHR1-3 domain in amphibian and reptile species that enables TRPM8 to undergo conformational changes at low temperatures. Furthermore, we found that the TRPM8 pore domain of terrestrial vertebrates evolved to tune the efficacy of cold activation, in which a cold-sensitive MHR1-3 domain is indispensable to achieve such a modulatory mechanism. Together, our findings suggest that the *trpm8* gene origination and formation of the TRPM8 MHR1-3 domain contributed to the transition of vertebrate life from water to land and that the efficacy of cold activation tuned by the TRPM8 pore domain diversified the setting of temperature-adaptive phenotypes in terrestrial vertebrates.

Results

The *trpm2* Gene–Derived *trpm8* in Lobe-Finned Fishes. Given that the *trpm8* gene can be observed in the whole genomes of amphibian and reptile species, while absent in those of 12 fish species from 10 different orders (14, 15, 21), we speculated that *trpm8* is necessary for modern tetrapods during the water-to-land transition (Fig. 1 *A*, *Left*). We therefore, established a phylogenetic tree, including representative ray- and lobe-finned fishes, amphibians, and reptiles to confirm the fixation of the *trpm8* gene (Fig. 1 *A*, *Right*). In ray-finned fishes, *trpm2* and *trpm2*-like genes with a high sequence identity locate at the same chromosome, where the fixation of *trpm8* gene loci can be found between *trpm2* and *trpm2*-like genes in lobe-finned fishes such as the African lungfish. Lungfishes can breathe air through the lungs and develop their fins with a limb-like structure (Fig. 1 *A*, *Left*), which are believed to be the important changes toward preadaptations for water-to-land transition. Consistently, although the loss of the *trpm2*-like gene is common in most amphibian and reptile species, the *trpm8* gene loci were retained close to the *trpm2* gene (Fig. 1*A*), suggesting the syntenic relationship among these genes. In the genome of the lungfish, more than 70% of the exons are highly conserved among *trpm2*, *trpm2*-like, and *trpm8* genes (*SI Appendix*, Fig. S1), and hence the gene duplication and exon shuffling process contributed to the origination of the *trpm8* gene (Fig. 1*B* and *SI Appendix*, Fig. S1). Although the animals involved in the transitional events are extinct, the origination of the *trpm8* gene in lobe-finned fishes suggests that the ability to sense environmental cold can be interpreted as one of the innovations associated with terrestrialization, due to a much faster response to radiative forcings observed in land temperature compared with oceanic temperature fluctuation (22).

Positive Selection of TRPM8 N Terminus in Fish–Tetrapod Evolution. To understand the functional evolution of the *trpm8* gene, we first tested the ligand sensitivity of several vertebrate TRPM8 orthologs using menthol, a well-recognized cooling compound that activates TRPM8 ion channels. Except for the lungfish TRPM8 (*Protopterus annectens*, PaTRPM8), all the orthologs from living amphibian and reptile species showed robust menthol-evoked currents, yielding half maximal effective concentration (EC_{50}) values ranging from 0.15 to 2.7 mM (*SI Appendix*, Fig. S2*A*). Among the TRPM8 orthologs, due to basic architecture and function, we assumed that the *trpm8* gene of the lungfish was retained in an earlier or more immature stage. In agreement with this idea, no response to the cold temperature of 8 °C was seen in PaTRPM8-expressing cells (Fig. 1*C*). We found that the TRPM8 orthologs (*Rhinatrema bivittatum*, RbTRPM8 and *Chelonia mydas*, CmTRPM8) of two species (caecilians and marine turtles) with menthol sensitivity also did not show activation upon cooling (*SI Appendix*, Fig. S2*A* and Fig. 1 *C* and *D*). This is interesting because caecilians are a highly distinctive species without limb-based locomotion that locate throughout the amphibian tree of life in early-branching anuran and salamander lineages (23). In addition, sea turtles are specialized open ocean cruisers with the most distinct morphological traits among turtle species and oceanic lifestyle, clustering away from semiaquatic and terrestrial turtles (24). Therefore, we speculated that the acquisition of cold sensitivity in TRPM8 might be related to the appearance of terrestrial tetrapods during the water-to-land transition. In addition, PaTRPM8, RbTRPM8, and CmTRPM8 possess unique evolutionary information, which might offer the opportunity to carry out a comparative study with other amphibian or reptile TRPM8 orthologs exhibiting cold activation (Fig. 1 *C* and *D* and *SI Appendix*, Fig. S2 *B* and *C*). We further employed Bayes empirical Bayes (BEB) testing to identify the residues under positive selection among five species (Fig. 1 *E*, *Top* and *SI Appendix*, Table S1), including a cold-sensitive TRPM8 ortholog (*Xenopus tropicalis*, XtTRPM8). In the structural diagram of XtTRPM8, we mapped nine residues under positive selection onto the channel and found that six of them are located at the N terminus (Fig. 1 *E*, *Bottom*). Although none of the residue substitutions on the six sites directly bestowed RbTRPM8 with cold activation (*SI Appendix*, Fig. S2*D*), the distribution of positive selection signals prompted us to test the contribution of the N terminus in cold sensitivity acquisition. Consistently, the N terminus, rather than other segments of XtTRPM8, bestowed RbTRPM8 with cold sensitivity (Fig. 1 *F* and *G* and *SI Appendix*, Fig. S2*E*), while these chimeric channels did not change menthol-induced activation (*SI Appendix*, Fig. S2*F*). The incorporation of the RbTRPM8 N terminus, as expected, disrupted the cold rather than the menthol sensitivity of XtTRPM8 (Fig. 1 *F* and *G* and *SI Appendix*, Fig. S2*F*). In addition, alanine substitution at the N terminus decreased the cold activation of XtTRPM8 (*SI Appendix*, Fig. S3). These results suggest that the evolution of the TRPM8 N terminus might promote low-temperature detection via cold-induced TRPM8 activation, thus facilitating adaptation to the diurnal temperature fluctuations in terrestrial environments.

Evolved MHR1-3 Domain Bestows TRPM8 with Cold Sensitivity. Because the maximum menthol-induced open probability of RbTRPM8 is around 12.6% (Fig. 2 *A* and *B*), we employed cold-insensitive CmTRPM8 with a robust menthol activation to further investigate the contribution of the N terminus in TRPM8 cold sensitivity. As expected, replacing the CmTRPM8 N terminus with the corresponding part of XtTRPM8 introduced discernible cold-induced activation (Fig. 2*C*). Given that four melastatin homology regions (MHRs) account for more than 90% of the N terminus in length, we constructed several chimeric channels following MHR structures to identify the apparatus within the N terminus that bestows TRPM8 with cold sensitivity (Fig. 2*C*). We found that the MHR1-2, MHR3, MHR4, or cytosolic

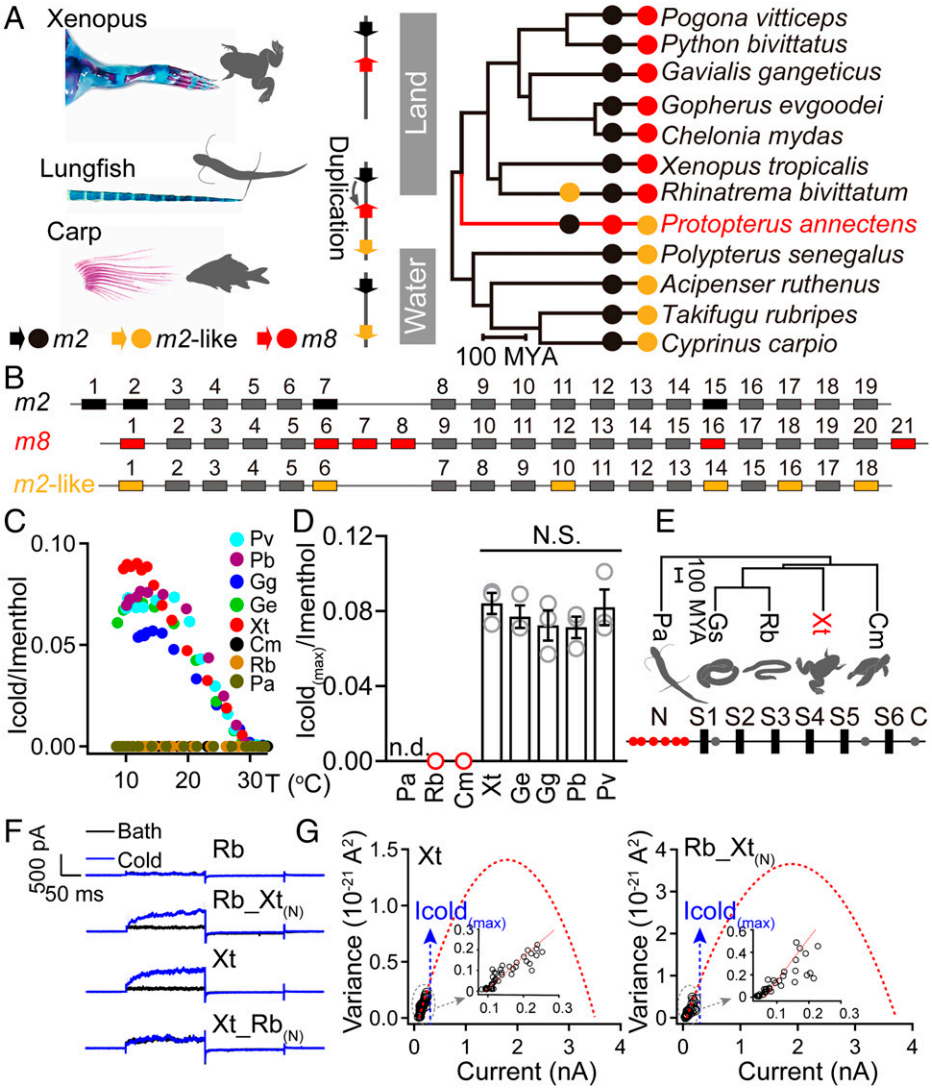

Fig. 1. The functional origination of *trpm8* genes. (*A*) To show the skeletal reconstruction (from pectoral fin to forelimb) of representative animals in water-to-land transition, bone and cartilage were stained in red (Alizarin red) and blue (Alcian blue), respectively. The location of *trpm2* (black), *trpm2*-like (yellow), and *trpm8* (red) genes on one of their chromosomes is indicated by solid arrows (*Left*). Phylogenetic relationships are shown among fishes, amphibians, and reptiles (*Right*). The presence or absence of *trpm2* (black), *trpm2*-like (yellow), and *trpm8* (red) genes is given. (*B*) Comparison of *trpm2*, *trpm8*, and *trpm2*-like gene structures in *P. annectens*. Solid boxes represent exons. Homologous exons are aligned and colored in gray. By comparing these exons of the three genes, the exons without sequence similarity are colored in black (*trpm2*), red (*trpm8*), or yellow (*trpm2*-like). (*C*) Representative temperature-driven activation of TRPM8 orthologs. The cold-activated currents were normalized to saturating menthol-induced activation at room temperature. (*D*) The maximum cold-induced activation of TRPM8 orthologs was normalized to the current amplitude induced by saturating menthol. Data are given as average ± SEM, $n = 3$. n.d., no data for the TRPM8 orthologs without menthol sensitivity; N.S., no significance. (*E*) Phylogenetic relationships among *P. annectens* (Pa), *Geotrypetes seraphini* (Gs), *R. bivittatum* (Rb), *X. tropicalis* (Xt), and *C. mydas* (Cm) (*Top*). The species highlighted in red represent the *trpm8* gene under significant positive selection. Positive selection sites on TRPM8 are shown as dots in a structural diagram (*Bottom*). Dots within the N-terminal of TRPM8 are shown in red. (*F*) Representative TRPM8 currents activated by cold bathing solution (8 °C). $Rb\_Xt_{(N)}$ represents RbTRPM8 N-terminal substituted by the homologous region of XtTRPM8, and vice versa [$Xt\_Rb_{(N)}$]. (*G*) Variance versus average current plot from TRPM8 current traces activated at different temperatures. The open probability was determined as the ratio between the macroscopic current (after correcting for temperature-dependent single-channel conductance) and the maximum current estimated using noise analysis.

pre-S1 domain from XtTRPM8 failed to independently enable CmTRPM8 to respond to cold temperatures, while the chimeric CmTRPM8 with both MHR1-2 and MHR3 of XtTRPM8 (CmTRPM8_XtMHR1-3) exhibited discernible cold-induced activation like wild-type XtTRPM8 (Fig. 2*C*). According to these observations, MHR1-2 and MHR3 were considered as a functionally combined domain (MHR1-3) in this study for further chimeric channel construction. Importantly, swapping the MHR1-3 domain of any cold-sensitive TRPM8 ortholog induced cold activation in these chimeric CmTRPM8s without affecting their response to menthol (Fig. 2 *D* and *G*). Vice versa, we found that the incorporation of the CmTRPM8 MHR1-3 domain disrupted the cold rather than menthol response of cold-sensitive TRPM8 orthologs (Fig. 2 *E* and *G*), whereas the MHR1-3 domains of cold-sensitive TRPM8 orthologs maintained their response to cold temperatures when swapped between each other (Fig. 2 *F* and *G*). In support of the MHR1-3 domain being an evolutionary module for TRPM8 cold sensitivity, these results show functional evidence by evaluating the electrophysiological properties of TRPM8 chimeras.

Evolved MHR1-3 Is an Independent Apparatus with Cold Sensitivity. We next questioned whether MHR1-3 could undergo conformational changes upon cooling. Given that multiple submolecular rearrangements may occur in diffuse areas during TRPM8 cold activation, we first constructed plasmids to express

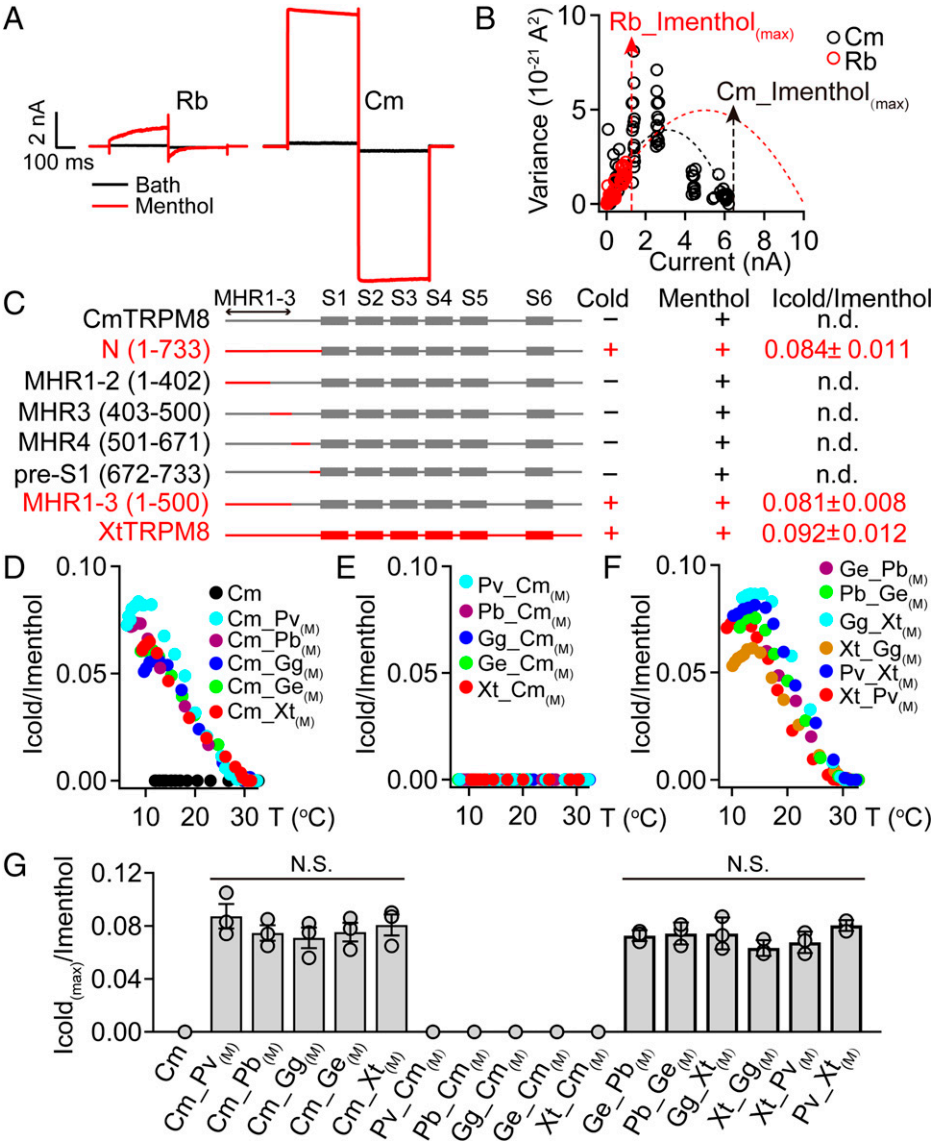

Fig. 2. The evolved MHR1-3 domain bestows TRPM8 orthologs with cold sensitivity. (*A*) Representative TRPM8 currents activated by 5 mM menthol. Rb, *R. bivittatum*; Cm, *C. mydas*. (*B*) Variance versus average current plots from TRPM8 currents activated by menthol at different concentrations. Open probability was determined as the ratio between the macroscopic current and the maximum current estimated using noise analysis. (*C*) Schematic representation of the chimeras (using CmTRPM8 amino acid number) between CmTRPM8 (gray) and XtTRPM8 (red). The responses of chimeras to cold and menthol are shown (n.d., no data for the channels without menthol sensitivity). (*D–F*) Representative temperature-driven activation of wild-type TRPM8 orthologs and chimeric channels. The chimeric channels are named X1_X2. X represents the species-specific TRPM8 orthologs. $X1\_X2_{(M)}$ represents the chimeric channel that the MHR1-3 domain of X1TRPM8 was substituted by the homologous region of X2TRPM8. The cold-activated currents were normalized to saturating menthol-induced activation. (*G*) Summary of the maximum cold response in wild-type TRPM8 orthologs and the chimeric channels (average ± SEM; $n = 3$; N.S., no significance).

each separated domain, including MHR1-3, MHR4, and pre-S1. By incorporating a fluorescence unnatural amino acid 3-(6-acetylnaphthalen-2-ylamino)-2-aminopropanoic acid (ANAP) (*SI Appendix*, Fig. S4*A*), the conformational changes of these domains could be reported by the shifts in emission peak of ANAP (25). We incorporated ANAP at 35 sites throughout the N terminus of XtTRPM8 and found that five mutants (P166ANAP, I360ANAP, D413ANAP, L453ANAP, and L537ANAP) exhibited a significant shift in their ANAP emission peaks upon cooling (*SI Appendix*, Fig. S4*B*). As detailed in Fig. 3*A*, ANAP substitution at four sites (P166ANAP, I360ANAP, L453ANAP, and L537ANAP) exhibited a remarkable redshift in emission peak, while it showed a striking blueshift at the position of D413 (D413ANAP). Interestingly, these mutated sites were clustered in the MHR1-3 rather than MHR4 and pre-S1 domains (Fig. 3*A*), implying that such a movement in MHR1-3 may exert a force on surrounding structures in the cold-induced activation of XtTRPM8. To test whether these sites are sufficient to indicate the dynamics of the isolated MHR1-3 domain during cold activation, we further incorporated ANAP at these homologous positions in species-specific MHR1-3. We found that the shifted ANAP emission signals successfully reported the conformational changes of MHR1-3 from the cold-sensitive TRPM8 orthologs (*SI Appendix*, Fig. S4*C*). In contrast, none of the ANAP signal change exceeded the threshold (4 nm) in two functional TRPM8 orthologs without cold-induced channel opening (*SI Appendix*, Fig. S4*C*). Although the ANAP fluorescence directly probed the side-chain microenvironmental state of a certain position, it is also necessary to evaluate whether the global structure undergoes temperature-dependent dynamics. By controlling the column temperature of a gel permeation chromatography, MHR1-3 of XtTRPM8, but not that of CmTRPM8, exhibited different

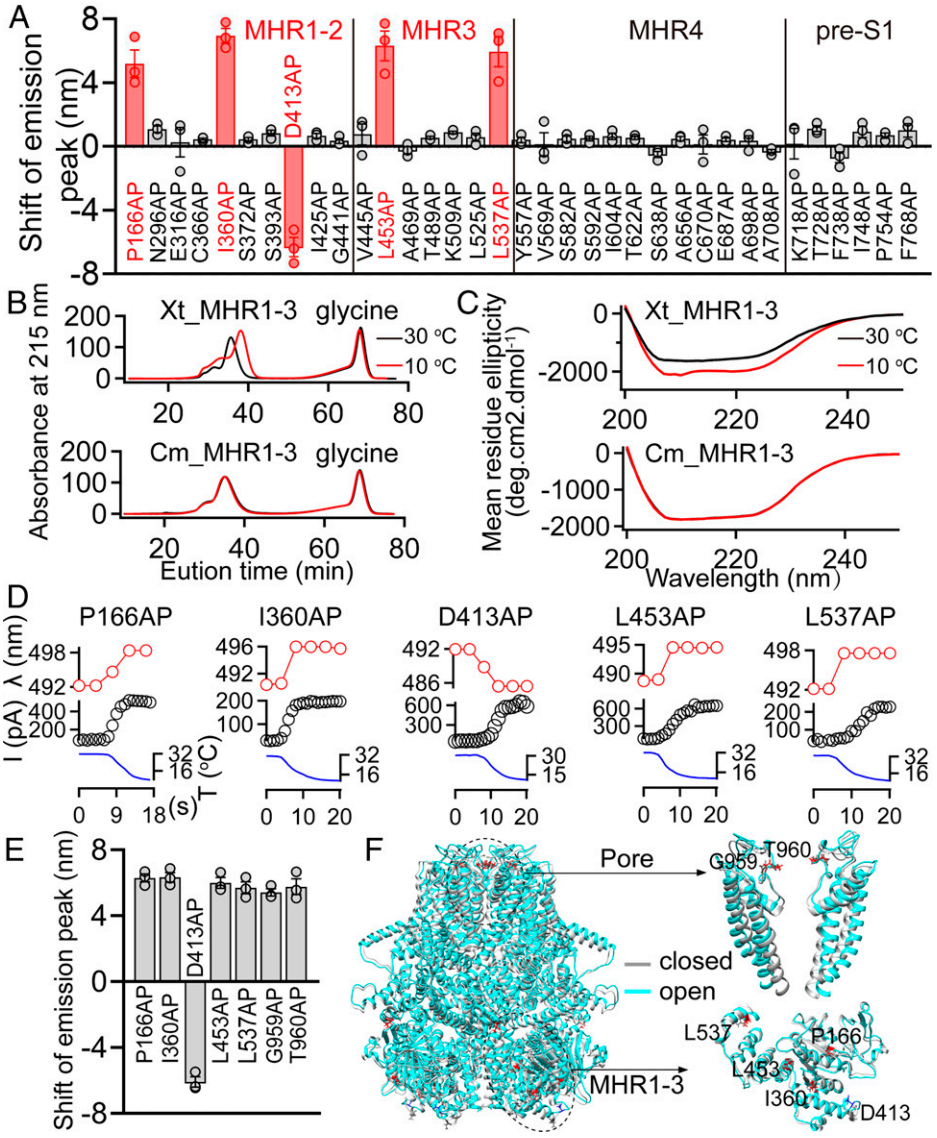

Fig. 3. The MHR1-3 domain exhibits conformational changes upon cooling. (*A*) Summary of the shifts in emission peak of ANAP mutants in each domain (average ± SEM; $n = 3$). The columns colored in red represent the ANAP emission peak shifted significantly upon cooling (larger than 4 nm). AP represents the ANAP substitution. (*B*) Gel filtration chromatography of the MHR1-3 domain of XtTRPM8 (*Top*) or CmTRPM8 (*Bottom*). The temperatures of the column are given. Glycine was used as a control. (*C*) Circular dichroism (CD) spectra of the MHR1-3 domain of XtTRPM8 (*Top*) or CmTRPM8 (*Bottom*) at cold (10 °C) and moderate temperature (30 °C), respectively. (*D*) Representative currents and the ANAP emission peak induced by a temperature ramp were recorded from HEK293 cells expressing ANAP-incorporated XtTRPM8. (*E*) Summary of the shifts in emission peak of ANAP mutants in full-length XtTRPM8 (average ± SEM; $n = 3$). (*F*) Structural alignment of the XtTRPM8 model in the close state (gray) and cold-activated state (cyan). The pore region (S5–S6 segment) and MHR1-3 domain exhibited discernible conformational rearrangements between these two states. The key sites with the shifts in emission peak of ANAP are shown in these structures.

retention times at 30 °C and 10 °C (Fig. 3*B*). Consistently, we found that decreasing the temperature significantly altered the secondary structural features of XtTRPM8 MHR1-3 but not CmTRPM8 MHR1-3 (Fig. 3*C*). More importantly, we simultaneously recorded the ANAP signals and currents on full-length XtTRPM8 to test whether these sites determined by the isolated domain assay also underwent similar conformational changes during the cold activation of TRPM8. A substantial change in ANAP emission at each of these sites was observed when the channels transitioned from the closed state to the cold-activated state (Fig. 3*D* and *SI Appendix*, Fig. S4*D*). With constraints of the residues with shifted ANAP emission peak (Fig. 3*E*) and multiple rounds of kinematic loop modeling, we computationally modeled XtTRPM8 structures at both the closed and cold-activated states (Fig. 3*F* and *SI Appendix*, Fig. S5*A*). By comparing these models, we found that the conformation of the MHR1-3 domain is significantly changed during TRPM8 cold activation (Fig. 3*F*). Furthermore, the significant change in solvent-accessible surface area (SASA) of the five sites was also observed during the gating transition of TRPM8 cold activation (*SI Appendix*, Fig. S5 *B* and *C*). These observations together suggest that the MHR1-3 that independently displays different conformation upon cooling is a functional apparatus in species-specific TRPM8, thus correlating to the cold sensitivity of TRPM8 orthologs.

Positive Selection of the Pore Domain in Mammalian TRPM8. To echo our previous finding that residues (especially residue 919 in African elephant TRPM8) in the pore domain also play a role in tuning the cold activation of TRPM8 (8), we first tested the sites under positive selection among TRPM8 proteins from terrestrial tetrapods with cold activation. Nine sites of camel TRPM8 (CbTRPM8), including residue 915 (the homologous

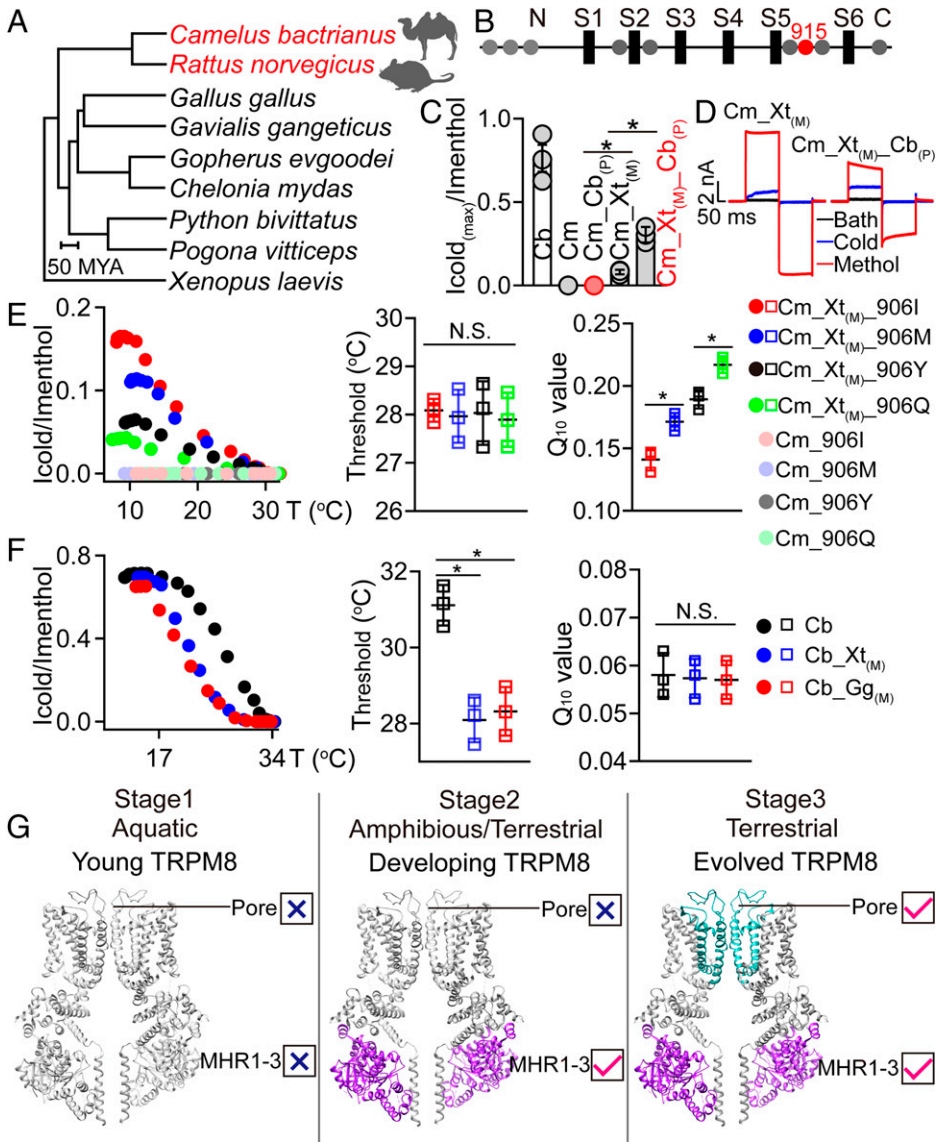

Fig. 4. The evolved MHR1-3 domain is required for pore domain function in tuning cold activation. (*A*) Phylogenetic relationship of TRPM8 orthologs with cold activation. The species-specific TRPM8s under significant positive selection are shown in red. (*B*) Positive selection sites of TRPM8 observed in *Camelus bactrianus* and *Rattus norvegicus* were mapped on a structural diagram of TRPM8. The residue 915 (in CbTRPM8 number) is highlighted in red. (*C*) Normalized maximum cold-induced currents of CmTRPM8 and the chimeric channels (average ± SEM; $n = 3$). The chimeric channels are named as X1_X2. X represents the species-specific TRPM8. X1_X2$_{(p)}$ means the chimeric channel that the pore domain of X1TRPM8 was substituted by the homologous region of X2TRPM8. X1_X2$_{(M)}$_X3$_{(p)}$ means that the MHR1-3 and pore domain of X1TRPM8 were substituted by the MHR1-3 domain of X2TRPM8 and the pore domain of X3TRPM8, respectively. The chimeric channels based on CmTRPM8 were constructed by homologous recombination using the Xt$_{(M)}$ segment (1 to 540, in XtTRPM8 number) and/or the Cb$_{(P)}$ segment (856 to 976, in CbTRPM8 number). (*D*) Representative currents of chimeric TRPM8 channels activated by cold bathing solution (8 °C) and 5 mM menthol. (*E*) Representative temperature-driven activation of CmTRPM8 point mutations (residue 906, in CmTRPM8 number) with or without the MHR1-3 domain of XtTRPM8. The cold-activated currents were normalized to saturating menthol-induced activation (*Left*). Temperature threshold of the chimeric channels is shown with the MHR1-3 domain of XtTRPM8 (*Middle*). Q_{10} value of the chimeric channels is shown (*Right*). Data are given as average ± SEM, $n = 3$, *$P < 0.01$. N.S., no significance. (*F*) Representative temperature-driven activation of CbTRPM8 and chimeric channels (*Left*). Temperature threshold (*Middle*) and Q_{10} value (*Right*) of CbTRPM8 and chimeric channels. Data are given as average ± SEM, $n = 3$, *$P < 0.01$. (*G*) The summary of TRPM8 functional evolution. The cryo-electron microscopy structure of TRPM8 (PDB: 6O77) was used (38).

site of residue 919 in our previous report) showed remarkable selection signals by using BEB testing (Fig. 4 *A* and *B* and *SI Appendix*, Table S2). The distribution of selection signals implies that mutations in the TRPM8 pore domain amassed later than that in the MHR1-3 domain throughout evolution. Based on the understanding of MHR1-3, we were prompted to investigate the relationship between the pore domain and MHR1-3 from the perspective of the gating mechanism. As illustrated in Fig. 4*C*, CbTRPM8 exhibited robust cold-induced activation, while its pore domain failed to bestow CmTRPM8 with cold sensitivity. Interestingly, once CmTRPM8 acquired cold-induced gating by swapping XtTRPM8 MHR1-3, further replacement of the pore domain on such a chimera could largely promote the efficacy of cold activation (Fig. 4 *C* and *D*). Since altering the side-chain hydrophobicity at residue 919 (amino acid number according to African elephant TRPM8) led to specific tuning of the efficacy of cold activation (8), we tested whether such a functional regulation by single mutation also requires an evolved MHR1-3 domain. Please note that the homologous site in CmTRPM8 is 906. Similarly, no discernible cold activation was observed in CmTRPM8 by increasing the side-chain hydrophobicity at residue 906 (Fig. 4 *E*, *Left*). Based on the chimeric CmTRPM8 incorporated by XtTRPM8 MHR1-3, changing the side-chain hydrophobicity of residue 906 significantly altered the efficacy of cold activation as

well as the sensitivity to temperature changes, while these substitutions had no obvious effect on temperature threshold (Fig. 4*E* and *SI Appendix*, Fig. S6). Furthermore, swapping the MHR1-3 domain was sufficient to alter the temperature threshold, but not the robustness of the cold response (Fig. 4*F*). From the perspective of channel gating, these findings suggest that the cold sensitivity established by MHR1-3 serves as the prerequisite for the regulatory mechanism of the pore domain in TRPM8 cold activation. In combination with the independent cold sensitivity of MHR1-3, the conformational changes are expected to induce pore gating during TRPM8 cold activation.

Discussion

The hard fossil evidence that shows the stages of Phanerozoic water-to-land transition events has received enormous attention in the field of biology. But what sophisticated functions are aquatic animals equipped with that have enabled them to adapt to such an extreme habitat shift? Although small and fragmentary fossils have indicated many aspects of fish–tetrapod transition (26, 27), there is a wide array of changes in both morphology and function for terrestrial adaptation that we can infer from the fossil record to understand this transition, one of the greatest steps in vertebrate history. Unexpectedly, our study suggested a strong correlation among *trpm8* gene formation, the appearance of TRPM8 cold activation, and terrestrial adaptation. The *trpm8* found in lobe-finned fishes can be considered as the intermediate type without cold sensitivity at the protein level (Fig. 1 *C* and *D*). Our results emphasize the importance of MHR1-3 evolution under positive selection that enabled the domain to respond to low temperatures, which further allowed semiaquatic and terrestrial species to possess the TRPM8 channel with cold-induced gating. Importantly, MHR1-3 from cold-insensitive TRPM8 orthologs barely rearranged in different temperatures, while those from cold-sensitive TRPM8s exhibited discernible conformational change upon cooling (Fig. 3 and *SI Appendix*, Fig. S4 *A–C*). Although the domains, residues, and atoms likely contribute to the thermodynamic properties simultaneously, swapping results (Fig. 2) strongly suggest that MHR1-3 acts as a unique domain required for thermosensation in *trpm8* gene evolution. Due to the exclusive monophyly of extant marine turtles compared with the nonmarine lineages (24), the sea turtle's TRPM8 likely underwent a functional loss of cold activation and possessed a cold-insensitive MHR1-3 domain. Although the *trpm8* gene arose in the lungfish's genome, intriguingly, the cold sensitivity of TRPM8 is absent in tested aquatic species (lungfish, marine turtle, and caecilian), while likely equipped by all semiaquatic amphibians and turtles. Given the higher effective heat capacity of water compared with that of land, ambient temperature fluctuations are much more severe in the terrestrial environment. Despite the direct heat exchange, the heat loss by evaporation further accelerates the change in body temperature of terrestrial species. In this sense, the acquisition of cold sensitivity in TRPM8 is necessary for detecting a rapid drop either in ambient or body temperature, which is barely essential in aquatic lifestyle. Therefore, we prefer the idea that the cold-sensitive TRPM8 updated the system of molecular thermometers during the water-to-land transition, which is expected to be an essential prerequisite for terrestrial adaptation.

Among the known major functional changes (27–30), recent studies highlighted sensory system innovations for terrestrial adaptation or preadaptation, including olfactory, visual, auditory, and gustatory sensations (31–35). How the ancestors of tetrapods coped with fluctuating temperature on land seems to be neglected. As discussed above, we assume that the establishment of an acute cold sensation contributed to the adaptive trait for land surface and air temperature fluctuations. Accordingly, the cold-sensitive TRPM8 orthologs in semiaquatic amphibians and reptiles contain a well-evolved MHR1-3 domain, although these animals are mostly confined to aquatic and relatively mesic terrestrial environments. In support of MHR1-3 being a functional domain with independent thermosensitivity (Fig. 3), swapping the MHR1-3 domain among cold-sensitive TRPM8 orthologs was sufficient to alter the temperature threshold, but not the robustness of the cold response (Fig. 4*F*). Based on the formation of a cold-sensitive MHR1-3 domain, further mutations clustered in the pore domain under positive selection can be identified among terrestrial vertebrates. In functional tests, we found that the tuning of efficacy of cold activation by swapping the pore domain required an evolved MHR1-3 domain in TRPM8 orthologs (Fig. 4 *C–E*). These observations suggest that the pore domain unlikely serves as an actual "temperature sensor" in the temperature-gating mechanisms of TRPM8. Coincidently, our previous study showed that mutations in the pore domain could tune the efficacy of open probability rather than abolish the cold sensitivity of TRPM8 (8). For semiaquatic and terrestrial species, the amino acid sequences of the pore regions were diverse in these cold-sensitive TRPM8 orthologs to match species-specific habitat temperature. Therefore, the cold activation of TRPM8 likely underwent a two-step model to achieve functional diversity: 1) The cold-sensitive MHR1-3 domain located in the N terminus was established during the water-to-land transition, which bestowed the channel with cold sensitivity; and 2) terrestrial animals possessing cold-sensitive TRPM8 tuned the maximum cold activation by altering the configurational properties of the pore domain (Fig. 4*G*). In combination with the evolutionary and functional relationships between MHR1-3 and the pore domain of TRPM8, our findings strongly implicate that the MHR1-3 domain serves as a thermosensitive region required for the cold sensitivity of TRPM8, and that the MHR1-3 conformational changes likely lead to the pore opening during TRPM8 cold activation. Furthermore, biophysical efforts will hopefully pinpoint the physical coupling of these two evolutionary units in the future.

Materials and Methods

A full description of materials and methods is available in *SI Appendix*.

Gene Prediction and Comparison. The *trpm2*, *trpm2*-like, and *trpm8* genes in *P. annectens* were predicted and annotated from the full genome (National Genomic Data Center Accession No. GWHANVS00000000) by the GeneWise sequence analysis tool (36). Coding sequence comparison of *trpm2*, *trpm8*, and *trpm2*-like genes was performed using VISTA tools (37).

Data Availability. All study data are included in the article and/or supporting information.

ACKNOWLEDGMENTS. This project was supported by grants from the National Natural Science Foundation of China (32022010 and 32170486), the National Forestry and Grassland Administration (2020132610), and Heilongjiang Province (JQ2021C001) (to S.Y.); the National Natural Science Foundation of China (32100372) and the Fundamental Research Funds for the Central Universities (2572021DQ07) (to X.L.); and the National Natural Science Foundation of China (32000310) and Heilongjiang Province (YQ2021H001) (to Y.W.).

Author affiliations: [a]College of Wildlife and Protected Area, Northeast Forestry University, 150040 Harbin, China; [b]Key Laboratory of Animal Models and Human Disease Mechanisms, Chinese Academy of Sciences, Kunming, 650223 China; and [c]Key Laboratory of Bioactive Peptides of Yunnan Province, Kunming Institute of Zoology, Chinese Academy of Sciences, 650223 Kunming, China

1. A. Patapoutian, A. M. Peier, G. M. Story, V. Viswanath, ThermoTRP channels and beyond: Mechanisms of temperature sensation. *Nat. Rev. Neurosci.* **4**, 529–539 (2003).
2. M. J. Caterina *et al.*, The capsaicin receptor: A heat-activated ion channel in the pain pathway. *Nature* **389**, 816–824 (1997).
3. M. J. Caterina *et al.*, Impaired nociception and pain sensation in mice lacking the capsaicin receptor. *Science* **288**, 306–313 (2000).
4. D. D. McKemy, W. M. Neuhausser, D. Julius, Identification of a cold receptor reveals a general role for TRP channels in thermosensation. *Nature* **416**, 52–58 (2002).
5. E. O. Gracheva *et al.*, Ganglion-specific splicing of TRPV1 underlies infrared sensation in vampire bats. *Nature* **476**, 88–91 (2011).
6. E. O. Gracheva *et al.*, Molecular basis of infrared detection by snakes. *Nature* **464**, 1006–1011 (2010).
7. L. Luo *et al.*, Molecular basis for heat desensitization of TRPV1 ion channels. *Nat. Commun.* **10**, 2134 (2019).
8. S. Yang *et al.*, A paradigm of thermal adaptation in penguins and elephants by tuning cold activation in TRPM8. *Proc. Natl. Acad. Sci. U.S.A.* **117**, 8633–8638 (2020).
9. W. J. Laursen, E. R. Schneider, D. K. Merriman, S. N. Bagriantsev, E. O. Gracheva, Low-cost functional plasticity of TRPV1 supports heat tolerance in squirrels and camels. *Proc. Natl. Acad. Sci. U.S.A.* **113**, 11342–11347 (2016).
10. L. J. Hoffstaetter, S. N. Bagriantsev, E. O. Gracheva, TRPs et al.: A molecular toolkit for thermosensory adaptations. *Pflugers Arch.* **470**, 745–759 (2018).
11. A. M. Peier *et al.*, A TRP channel that senses cold stimuli and menthol. *Cell* **108**, 705–715 (2002).
12. A. Dhaka *et al.*, TRPM8 is required for cold sensation in mice. *Neuron* **54**, 371–378 (2007).
13. D. M. Bautista *et al.*, The menthol receptor TRPM8 is the principal detector of environmental cold. *Nature* **448**, 204–208 (2007).
14. B. R. Myers, Y. M. Sigal, D. Julius, Evolution of thermal response properties in a cold-activated TRP channel. *PLoS One* **4**, e5741 (2009).
15. E. O. Gracheva, S. N. Bagriantsev, Evolutionary adaptation to thermosensation. *Curr. Opin. Neurobiol.* **34**, 67–73 (2015).
16. S. Brauchi, G. Orta, M. Salazar, E. Rosenmann, R. Latorre, A hot-sensing cold receptor: C-terminal domain determines thermosensation in transient receptor potential channels. *J. Neurosci.* **26**, 4835–4840 (2006).
17. T. Voets *et al.*, The principle of temperature-dependent gating in cold- and heat-sensitive TRP channels. *Nature* **430**, 748–754 (2004).
18. V. Matos-Cruz *et al.*, Molecular prerequisites for diminished cold sensitivity in ground squirrels and hamsters. *Cell Rep.* **21**, 3329–3337 (2017).
19. M. Pertusa, B. Rivera, A. González, G. Ugarte, R. Madrid, Critical role of the pore domain in the cold response of TRPM8 channels identified by ortholog functional comparison. *J. Biol. Chem.* **293**, 12454–12471 (2018).
20. K. Wang *et al.*, African lungfish genome sheds light on the vertebrate water-to-land transition. *Cell* **184**, 1362–1376.e18 (2021).
21. F. Seebacher, S. A. Murray, Transient receptor potential ion channels control thermoregulatory behaviour in reptiles. *PLoS One* **2**, e281 (2007).
22. Z. Shen, Y. Ming, I. M. Held, Using the fast impact of anthropogenic aerosols on regional land temperature to constrain aerosol forcing. *Sci. Adv.* **6**, eabb5297 (2020).
23. J. D. Pardo, B. J. Small, A. K. Huttenlocker, Stem caecilian from the Triassic of Colorado sheds light on the origins of Lissamphibia. *Proc. Natl. Acad. Sci. U.S.A.* **114**, E5389–E5395 (2017).
24. B. V. Dickson, S. E. Pierce, Functional performance of turtle humerus shape across an ecological adaptive landscape. *Evolution* **73**, 1265–1277 (2019).
25. A. Chatterjee, J. Guo, H. S. Lee, P. G. Schultz, A genetically encoded fluorescent probe in mammalian cells. *J. Am. Chem. Soc.* **135**, 12540–12543 (2013).
26. J. L. Molnar, R. Diogo, J. R. Hutchinson, S. E. Pierce, Reconstructing pectoral appendicular muscle anatomy in fossil fish and tetrapods over the fins-to-limbs transition. *Biol. Rev. Camb. Philos. Soc.* **93**, 1077–1107 (2018).
27. I. Schneider, N. H. Shubin, The origin of the tetrapod limb: From expeditions to enhancers. *Trends Genet.* **29**, 419–426 (2013).
28. N. Shubin, C. Tabin, S. Carroll, Deep homology and the origins of evolutionary novelty. *Nature* **457**, 818–823 (2009).
29. N. Shubin, C. Tabin, S. Carroll, Fossils, genes and the evolution of animal limbs. *Nature* **388**, 639–648 (1997).
30. N. P. Kelley, N. D. Pyenson, Vertebrate evolution. Evolutionary innovation and ecology in marine tetrapods from the Triassic to the Anthropocene. *Science* **348**, aaa3716 (2015).
31. X. Bi *et al.*, Tracing the genetic footprints of vertebrate landing in non-teleost ray-finned fishes. *Cell* **184**, 1377–1391.e14 (2021).
32. B. Lu *et al.*, A large genome with chromosome-scale assembly sheds light on the evolutionary success of a true toad (*Bufo gargarizans*). *Mol. Ecol. Resour.* **21**, 1256–1273 (2021).
33. C. B. Christensen, J. Christensen-Dalsgaard, P. T. Madsen, Hearing of the African lungfish (*Protopterus annectens*) suggests underwater pressure detection and rudimentary aerial hearing in early tetrapods. *J. Exp. Biol.* **218**, 381–387 (2015).
34. N. S. Hart, H. J. Bailes, M. Vorobyev, N. J. Marshall, S. P. Collin, Visual ecology of the Australian lungfish (*Neoceratodus forsteri*). *BMC Ecol.* **8**, 21 (2008).
35. J. A. Long, M. S. Gordon, The greatest step in vertebrate history: A paleobiological review of the fish-tetrapod transition. *Physiol. Biochem. Zool.* **77**, 700–719 (2004).
36. F. Madeira *et al.*, The EMBL-EBI search and sequence analysis tools APIs in 2019. *Nucleic Acids Res.* **47**, W636–W641 (2019).
37. K. A. Frazer, L. Pachter, A. Poliakov, E. M. Rubin, I. Dubchak, VISTA: Computational tools for comparative genomics. *Nucleic Acids Res.* **32**, W273–W279 (2004).
38. M. M. Diver, Y. Cheng, D. Julius, Structural insights into TRPM8 inhibition and desensitization. *Science* **365**, 1434–1440 (2019).